Pure Appl. Chem., Vol. 81, No. 9, pp. 1635–1644, 2009.
doi:10.1351/PAC-CON-08-09-23

Interaction of UV radiation with DNA helices*

Dimitra Markovitsi

Francis Perrin Laboratory, CEA-CNRS URA 2453, 91191 Gif-sur-Yvette, France

Abstract: Recent experimental and theoretical investigations dealing with model DNA double helices, composed of either adenine–thymine (A–T) or guanine–cytosine (G–C) base pairs, and G quadruplexes shed some light on the excited states populated by photon absorption and their relaxation, energy transfer among bases, and one-photon ionization. These studies revealed that the Franck–Condon excited states of DNA helices cannot be considered as the sum of their monomeric constituents because electronic coupling induces delocalization of the excitation over a few bases. Energy transfer takes place via intraband scattering in less than 100 fs. The fluorescence lifetimes of DNA helices detected by fluorescence upconversion and corresponding mainly to $\pi\pi^*$ transitions are longer than that of an equimolar mixture of nucleotides; the only exception was observed for alternating G–C polymers. Moreover, nanosecond flash photolysis experiments showed that organization of bases within single and double helices may lead to a lowering of their ionization potential. Finally, the first determination regarding the time-scale needed for the formation of T dimers, the (6–4) adducts, was determined for the single strand $(dT)_{20}$.

Keywords: DNA; excitons; energy transfer; fluorescence spectroscopy; photochemistry.

INTRODUCTION

It is well established today that absorption of UV radiation by DNA bases induces photochemical reactions, which may lead to carcinogenic mutations [1]. Although the final products associated with the resulting DNA lesions have been characterized [2], very little is known about the primary processes preceding the photoreactions (excited states and reaction paths). This is mainly due to the complexity and fragility of the system.

From a photochemical point of view, DNA is a multichromophoric system undergoing dynamical conformational changes. It is composed of four types of chromophores (nucleotides in Fig. 1) arranged in a huge number of sequences rendering the analysis and rationalization of experimental data obtained from photochemical studies very delicate. Furthermore, time-resolved experiments with DNA in aqueous solution require excitation around 260 nm, which easily induces two-photon ionization of both the double helix and the solvent. Some of these problems may be overcome by using synthetic DNA helices with simple base sequences and developing specific experimental protocols [3].

*Paper based on a presentation at the XXIInd IUPAC Symposium on Photochemistry, 28 July–1 August 2008, Gothenburg, Sweden. Other presentations are published in this issue, pp. 1615–1705.

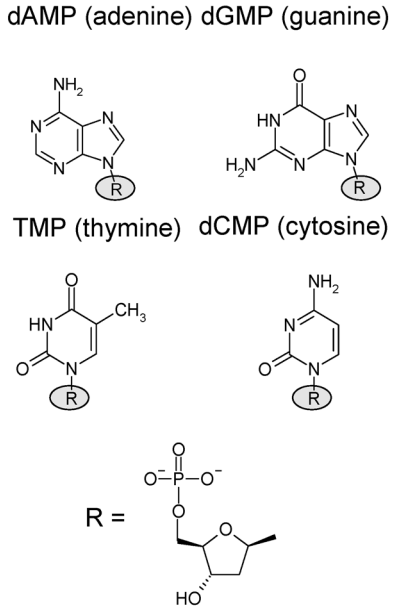

Fig. 1 DNA nucleotides: 2'-deoxyadenosine 5'-monophosphate (dAMP), thymidine 5'-monophosphate (TMP), 2'-deoxyguanosine 5'-monophosphate (dGMP), and 2'-deoxycytidine 5'-monophosphate (dCMP), corresponding to the bases: A, T, G, and C, respectively.

In this article, I will present a brief overview of the studies carried out in the Francis Perrin Laboratory on model DNA helices. We worked with simple helices containing 20 adenine (A) [$(dA)_{20}$] or thymine (T) [$(dT)_{20}$] residues, homopolymeric [$(dA)_n(dT)_n$] and alternating [$(dAdT)_n$·$(dAdT)_n$, $(dCdG)_n$·$(dCdG)_n$] double stands (Fig. 2), as well as quadruple helices containing only guanine (G) bases (G quadruplexes). I will refer to Franck–Condon states, energy transfer among bases, fluorescent states, one-photon ionization, and T dimer formation.

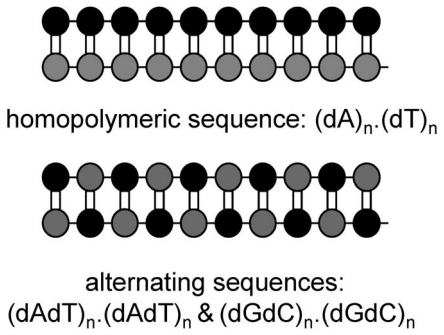

Fig. 2 Synthetic DNA double strands composed of only one type of base pairs: A–T [$(dA)_n(dT)_n$, $(dAdT)_n$·$(dAdT)_n$] or G–C [$(dGdC)_n$·$(dGdC)_n$].

FRANCK–CONDON STATES

Due to the electronic coupling, the excited states of a multichromophoric system may be delocalized over several chromophores. In particular, Franck–Condon states, associated with important oscillator strength, are subject to delocalization. Regarding DNA, Eisinger and Shulman remarked in 1968 that "The absorption spectrum of DNA closely resembles the sum of the absorption spectra of the constituent bases.[...]. The electronic interaction between the bases is weak enough so that it is proper to speak of the absorption of a UV photon by a single base" [4]. The hypothesis underlying such a statement is that the absorption spectrum associated with delocalized states is considerably shifted in energy compared to the spectrum of non-interacting chromophores. This was based on the conclusion of pioneering theoretical calculations published in the 1960s [5–7].

In the meantime, a better knowledge of the excited states of DNA nucleotides and the development of computational techniques gave the possibility to perform more precise calculations. Thus, we calculated the Franck–Condon states of the model double helices shown in Fig. 2 [8–11]. Our calculations were performed in the frame of the exciton theory combining data from molecular dynamics simulations, quantum chemistry, and taking into account the width of the experimental absorption spectra (Fig. 3).

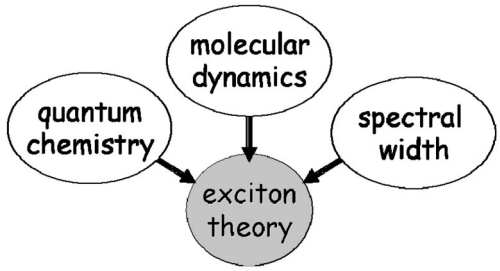

Fig. 3 The Franck–Condon excited states of model double helices were calculated in the frame of the exciton theory using data from quantum chemistry calculations, molecular dynamic simulations, and taking into account the width of experimental absorption spectra of nucleotides in solution.

Molecular dynamics calculations allowed us to determine various conformations of the studied helices in their ground state and examine how conformational changes affect the strength of electronic coupling (Fig. 4 in ref. [9]; Fig. 4 in ref. [11]). The electronic coupling between dipolar transitions was calculated by means of the atomic transition charges deduced from quantum chemistry methods. In this respect, we also demonstrated that the point dipole approximation overestimates the dipolar coupling in the case of close-lying bases within a helix [8]. Finally, the monomer energies were simulated by Gaussian functions resembling the absorption bands of nucleotides in aqueous solution [10,11].

The above theoretical studies showed that the absorption spectra of the helices largely overlap the spectra of non-interacting chromophores [10,11]. For example, the absorption maximum of $(dA)_{10}(dT)_{10}$ was found to be only a few nanometers shifted to higher energy with respect to the sum of the spectra of dAMP and TMP [10], in agreement with the experimental spectra [12]. Moreover, we did not find any visible splitting of the absorption band which is an envelop corresponding to a large number of transitions, associated with various conformations of the helix and vibrations of the monomeric units. This is illustrated in Fig. 4 where the degree of delocalization of the Franck–Condon excited states of $(dA)_{10}(dT)_{10}$, quantified by means of the participation ratio [13–15], is plotted as a function of their excitation energy. We observe that the excited states of the helix may extend over up to 8 bases and that the more delocalized states are located close to the absorption maximum.

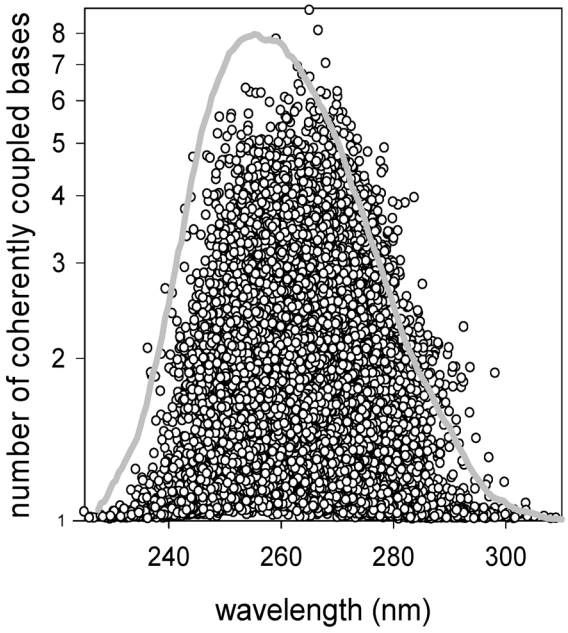

Fig. 4 The calculated absorption spectrum of $(dA)_{10}(dT)_{10}$ (gray) is an envelop of a large number of transitions. The circles represent the number of coherently coupled bases associated with each excited state as function of the excitation energy.

The maximum of the absorption band located around 260 nm determined experimentally for $(dA)_n(dT)_n$ is hypsochromically shifted compared to that of $(dAdT)_n{\cdot}(dAdT)_n$ (Fig. 5). Such a trend, predicted by the calculations [9], increases slightly when going from oligomers (440 cm^{-1} for $n = 20$) to polymers (550 cm^{-1} for $n > 200$) (Fig. 2 in ref. [3]). The observed difference was attributed to a decrease of conformational disorder with increasing the number of base pairs [16].

Our theoretical studies demonstrated that the dipolar coupling alone is capable of inducing delocalization of the excitation energy over a few bases within a DNA double strand even in the presence of conformational disorder and vibrational broadening. It should be stressed that other types of electronic interactions due to orbital overlap (charge resonance and charge transfer) operating between neighboring bases may also be quite important, but they are difficult to calculate for a double helix. Recent theoretical studies, performed for dimers of bases, dimers of base pairs, and short single strands [17,18], have shown that charge-transfer interactions do play an important role. In particular, these interactions are responsible for the so-called "DNA hypochromism". The difference in the oscillator strength between a double strand and the corresponding non-interacting chromophores depends on the base sequence. Figure 5 shows an example where the experimental spectra of poly(dA)·poly(dT) and poly(dAdT)·poly(dAdT) are presented together with the spectrum of an equimolar mixture of dAMP and TMP. It is worth noticing that the hypochromism, observed for these model helices from at least 200 to 280 nm, cannot be explained on the basis of exciton states induced by dipolar coupling.

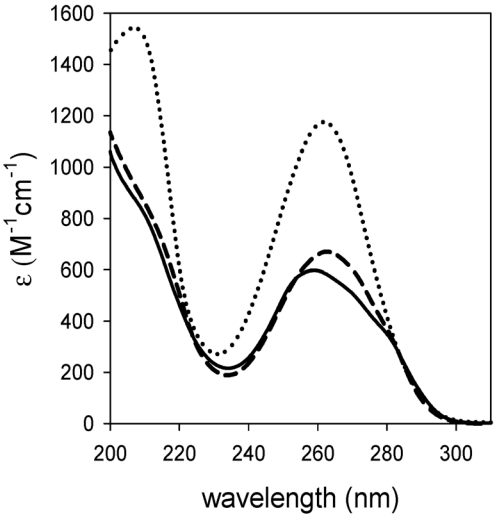

Fig. 5 Experimental absorption spectra of poly(dA)·poly(dT) (solid line), poly(dAdT)·poly(dAdT) (dashed line), and an equimolar mixture of dAMP and TMP.

ENERGY TRANSFER

The excited states of a double helix are, in general, characterized by different topographies. In other terms, each excited state is built on different electronic states of the monomeric chromophores (Fig. 9 in [8], Fig. 8 in [11]). Consequently, internal conversion among the states of the exciton band (intraband scattering) is expected to lead to energy transfer, as depicted schematically in Fig. 6.

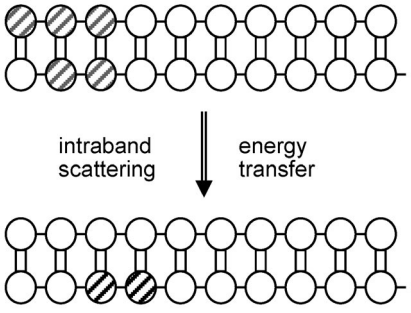

Fig. 6 Schematic representation of exciton states extended over five (top) and two (bottom) bases (hachured circles) of a double helix. Internal conversion among them results in a change in the location of the excitation energy.

By performing fluorescence measurements, we demonstrated that energy transfer does take place within a double strand. The case study was poly(dA)·poly(dT) [12,19], whose steady-state emission was known to be very similar to that of TMP [20]. This similarity had led to the conclusion that fluorescence arises from excited states localized on single T moieties [20]. We found that when the excitation wavelength ranges from 245 to 285 nm, not only the profile of the fluorescence spectrum (Fig. 2 in ref. [19]) but also the fluorescence quantum yield (3×10^{-4}) remain the same. The latter observation, associated to the fact that the two monomeric chromophores dAMP and TMP have quite different absorption and fluorescence spectra and different fluorescence quantum yields, allowed us to deduce that energy transfer between the two types of chromophores is very efficient.

We obtained further information about energy transfer in double strands from the time-dependence of the fluorescence anisotropy. To this end, we used femtosecond laser pulses at 267 nm and two different detection techniques, fluorescence upconversion and single-photon counting. We observed that the fluorescence anisotropy of TMP is close to the theoretical value 0.4. In contrast, the anisotropy of poly(dA)·poly(dT) is much lower. Its initial value is 0.28; after 1 ps, it drops down to 0.20 and becomes zero at about 1 ns [12]. This loss of anisotropy, too fast to be caused by physical rotation of such a large system (2000 base pairs), is a direct proof of energy transfer.

The scheme in Fig. 7 illustrates the energy flow in $(dA)_n(dT)_n$ deduced from our theoretical and experimental studies. Laser excitation at 267 nm populates a large number of states delocalized over a few bases. Intraband scattering, occurring in less than 100 fs, brings the system to the bottom of the exciton band. Emission arises from a large number of states, each one characterized by its own polarization, which is, in general, different than that of the Franck–Condon state (Fig. 10 in [9]). Ultrafast intraband scattering also accounts for the fact that the steady-state fluorescence spectra are independent of the excitation wavelength.

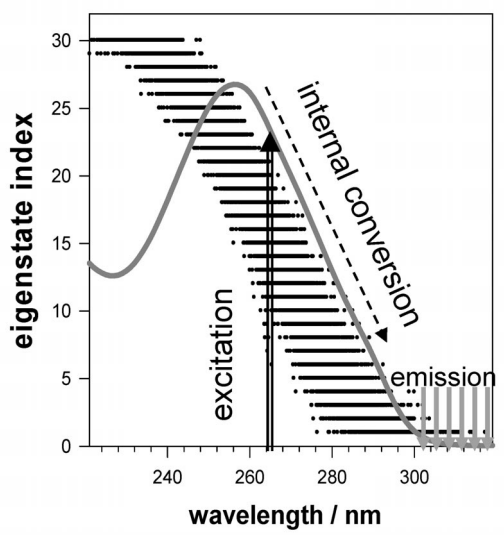

Fig. 7 Schematic representation of the excitation energy flow in $(dA)_n(dT)_n$. In gray: experimental absorption spectrum obtained for n = 2000. The 30 steps correspond to the excited state calculated for n = 10; the dots composing each step are associated with various conformations of the helix and vibration of the chromophores.

A decrease in the fluorescence anisotropy on the subpicosecond time-scale was observed for all the examined double strands, both oligomers and polymers [12,16,21,22]. Interestingly, the anisotropy values determined on the femtosecond time-scale for a polymer are lower than the corresponding value found for the oligomer with the same sequence. Figure 8 shows this effect in the case of homopolymeric and alternating A–T sequences $(dAdT)_n$·$(dAdT)_n$ and $(dA)_n(dT)_n$ (oligomers: n = 20; polymers: n > 200). Such a dependence on the size of the helix suggests that the collective behavior increases with the size of the helix and is line with the properties of the absorption spectra (Fig. 5).

It is possible that energy transfer continues at times longer that 1 ps. Recent theoretical studies calculated provide some insight into the survival probability of the initially formed excitons [23,24]. This process is expected to greatly depend on conformational motions.

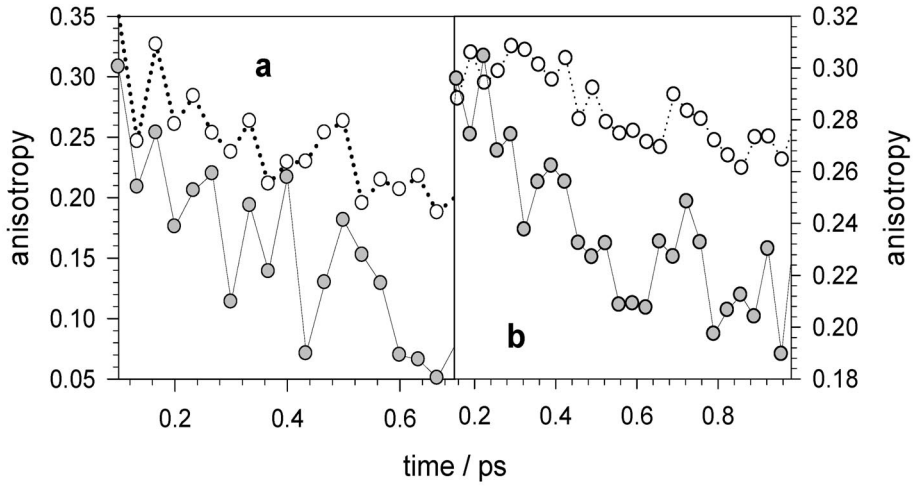

Fig. 8 Fluorescence anisotropy decays of oligomeric (open circles) and polymeric (gray circles) double strands: $(dAdT)_n \cdot (dAdT)_n$ (a) and $(dA)_n(dT)_n$ (b).

FLUORESCENT STATES

The decays detected by fluorescence upconversion for double helices composed of A–T pairs are, on average, slower than those detected for an equimolar mixture of dAMP and TMP [12,16–21]. This effect is more pronounced for polymers compared to the oligomers [16,21]. A slowing down of the fluorescence decays is also observed in the case of the single strands $(dA)_{20}$ and $(dT)_{20}$ compared to those of dAMP and TMP, respectively [25]. The same is true for a quadruple helix formed by self-association of four short single strands, tri-guanosine diphosphates; the fluorescence decay of this G quadruplex, containing only G bases is slower (4.7 ps) [26] by at least an order of magnitude than that of dGMP (0.34 ps) [27]. The behavior of alternating G–C double strands contrasts with the above-described trend. Indeed, the fluorescence decays of poly(dGdC)·poly(dGdC) detected by fluorescence upconversion are clearly faster than those of dGMP and dCMP [22]. An acceleration of the excited-state dynamics within G–C Watson–Crick dimers is predicted by theoretical studies which point out a proton transfer [28–30] occurring at the central hydrogen bond.

The electronic transitions associated with the decays which are monitored by fluorescence upconversion are characterized by strong transition moment (mainly $\pi\pi^*$ states). However, emission from less bright states can be detected by time-correlated single-photon counting. We reported such measurements for $(dA)_{20}(dT)_{20}$, $(dAdT)_{10}\cdot(dAdT)_{10}$, $(dA)_{20}$ [12,19,31]. Long-lived emitting states may be correlated with Frenkel excitons built on $\pi\pi^*$ states and corresponding to forbidden transitions, with charge-transfer states or with mixtures among them.

The existence of a variety of excited states is also supported by the strong dependence of the fluorescence lifetime with the emission wavelength and their extreme complexity. For example, in the case of poly(dA)·poly(dT), at least four time-constants are necessary to fit the decays recorded from 100 fs to 20 ns, and these "constants" vary with the emission wavelength [19]. Continuous conformational motions of the helices contribute to such an intricate picture because they alter the electronic coupling and, therefore, the properties of delocalized states.

ONE-PHOTON IONIZATION

The arrangement of the DNA bases in single and double strands not only affects the nature and the dynamics of the excited states but also may lead to a lowering of their ionization potential. The latter is a

key factor in the oxidative damage of DNA induced by various types of radiation and oxidizing agents [32]. Direct information about the photo-ionization process can be obtained by nanosecond flash photolysis, which allows the quantification of the generated hydrated electrons, characterized by broad absorption band peaking around 720 nm [33]. The sparse experiments of this type performed in the past for DNA oligomers and polymers in neutral pH had not detected one-photon ionization for excitation wavelengths greater than 210 nm [34–37].

We performed transient absorption experiments for $(dA)_{20}(dT)_{20}$, $(dAdT)_{10}$·$(dAdT)_{10}$, $(dA)_{20}$, and $(dT)_{20}$ in phosphate buffer (pH = 6.5) using nanosecond pulses at 267 nm with intensities lower than <1.3 MW/cm^2 [38]. A typical plot, obtained for $(dA)_{20}$, is presented in Fig. 9. It can be seen that the differential absorbance at 700 nm, divided by the laser intensity, varies linearly as a function of the laser intensity. The slope of the linear regression corresponds to a two-photon process, whereas the intercept on the ordinate is associated with one-photon ionization. Similar plots were obtained for $(dA)_{20}(dT)_{20}$ and $(dAdT)_{10}$•$(dAdT)_{10}$. The quantum yield of one-photon ionization deduced from these plots for the A-containing oligomers is of the order of 10^{-3}. No one-photon ionization was detected for $(dT)_{20}$.

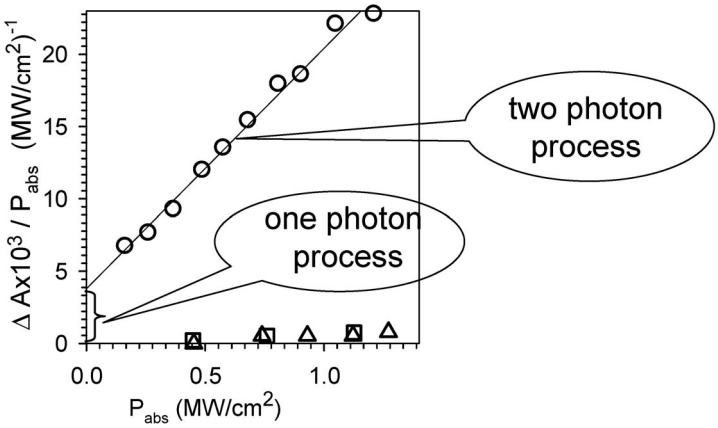

Fig. 9 Differential absorbance (700 nm; 200 ns) observed following laser excitation at 266 nm for $(dA)_{20}$ (circles) in phosphate buffer; dAMP buffered solutions (squares) and the buffer alone (triangles) gave negligible signals.

The hydrated electron disappears with a time-constant of 0.38 μs because it reacts efficiently with the phosphate ions present in high concentration in the buffer. The spectrum recorded for $(dA)_{20}(dT)_{20}$, $(dAdT)_{10}$•$(dAdT)_{10}$, and $(dA)_{20}$ at 2 μs resembles that of the deprotonated adenosine radical, suggesting that the positive charge in the double strands is located in the A moieties.

THYMINE DIMER FORMATION

The major photoproducts involved in the appearance of UV-induced carcinogenic mutations are pyrimidine dimers, cyclobutanes, and (6–4) adducts. In 2005, we reported the first study dealing with the time-scales on which such dimers are formed [39]. Our investigation was performed for the single-strand $(dT)_{20}$ using nanosecond flash photolysis with excitation at 266 nm. By probing the bleaching of the main absorption band at 290 nm, we showed that cyclobutane dimers are formed in less than 200 ns, which corresponds to the time-resolution of these experiments. This observation was recently confirmed by femtosecond studies [40,41].

In contrast to cyclobutanes, the formation of (6–4) adducts is much slower. As a matter of fact, the absorption band characteristic of these compounds, peaking at 325 nm, appears only on the millisecond time-scale (Fig. 10). The rise-time associated with this band was found to be 4 ms.

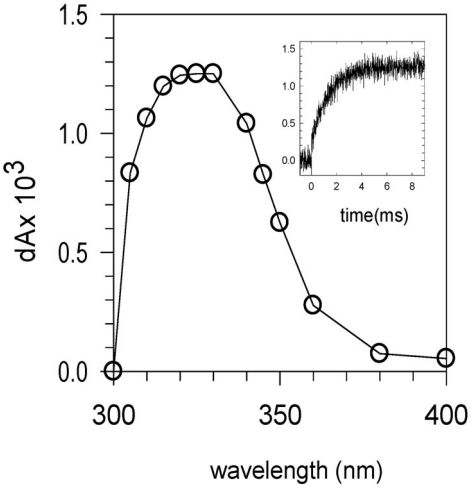

Fig. 10 Transient absorption spectrum recorded at 4 ms for $(dT)_{20}$ in phosphate buffer following excitation at 266 nm. The inset shows the rise-time at 325 nm.

ACKNOWLEDGMENTS

I gratefully acknowledge the contribution of my colleagues and coworkers who participated in this work: Akos Banyasz, Benjamin Bouvier, Delphine Onidas, Emanuela Emanuele, Thomas Gustavsson, Elodie Lazzarotto, Sylvie Marguet, François-Alexandre Miannay, Philippe Millié, Alexei Sharonov, and Francis Talbot from the Francis Perrin Laboratory; Richard Lavery and Krystyna Zakrzewska (Institut de Biologie et Chimie des Protéines, Lyon).

REFERENCES

1. N. Dumaz, H. J. Van Kranen, A. De Vries, R. J. W. Berg, P. W. Wester, C. F. Van Kreijl, A. Sarasin, L. Daya-Grosjean, F. R. De Gruijl. *Carcinogenesis* **18**, 897 (1997).
2. J.-L. Ravanat, T. Douki, J. Cadet. *J. Photochem. Photobiol., B* **63**, 1011 (2001).
3. D. Markovitsi, D. Onidas, F. Talbot, S. Marguet, T. Gustavsson, E. Lazzarotto. *J. Photochem. Photobiol., A* **183**, 1 (2006).
4. J. Eisinger, R. G. Shulman. *Science* **161**, 1311 (1968).
5. I. Tinoco Jr. *J. Am. Chem. Soc.* **82**, 4785 (1960).
6. W. Rhodes. *J. Am. Chem. Soc.* **83**, 3609 (1961).
7. T. Miyata, S. Yomosa. *J. Phys. Soc. Jpn.* **27**, 727 (1969).
8. B. Bouvier, T. Gustavsson, D. Markovitsi, P. Millié. *Chem. Phys.* **275**, 75 (2002).
9. B. Bouvier, J. P. Dognon, R. Lavery, D. Markovitsi, P. Millié, D. Onidas, K. Zakrzewska. *J. Phys. Chem. B* **107**, 13512 (2003).
10. E. Emanuele, D. Markovitsi, P. Millié, K. Zakrzewska. *ChemPhysChem* **6**, 1387 (2005).
11. E. Emanuele, K. Zakrzewska, D. Markovitsi, R. Lavery, P. Millie. *J. Phys. Chem. B* **109**, 16109 (2005).

12. D. Markovitsi, D. Onidas, T. Gustavsson, F. Talbot, E. Lazzarotto. *J. Am. Chem. Soc.* **127**, 17130 (2005).
13. S. Marguet, D. Markovitsi, P. Millié, H. Sigal, S. Kumar. *J. Phys. Chem. B* **102**, 4697 (1998).
14. P. Dean. *Rev. Mod. Phys.* **44**, 127 (1972).
15. M. Schreiber, Y. Toyosawa. *J. Phys. Soc. Jpn.* **51**, 1537 (1982).
16. D. Onidas, T. Gustavsson, E. Lazzarotto, D. Markovitsi. *J. Phys. Chem. B* **111**, 9644 (2007).
17. E. B. Starikov. *Mod. Phys. Lett. B* **18**, 825 (2004).
18. F. Santoro, V. Barone, R. Improta. *Proc. Natl. Acad. Sci. USA* **104**, 9931 (2007).
19. D. Markovitsi, T. Gustavsson, F. Talbot. *Photochem. Photobiol. Sci.* 717 (2007).
20. G. Ge, S. Georghiou. *Photochem. Photobiol.* **54**, 477 (1991).
21. D. Onidas, T. Gustavsson, E. Lazzarotto, D. Markovitsi. *Phys. Chem. Chem. Phys.* **9**, 5143 (2007).
22. F. A. Miannay, A. Banyasz, T. Gustavsson, D. Markovitsi. *J. Am. Chem. Soc.* **129**, 14574 (2007).
23. E. R. Bittner. *J. Chem. Phys.* **125**, 094909 (2006).
24. E. R. Bittner. *J. Photochem. Photobiol., A* **190**, 328 (2007).
25. D. Markovitsi, A. Sharonov, D. Onidas, T. Gustavsson. *ChemPhysChem* **3**, 303 (2003).
26. D. Markovitsi, T. Gustavsson, A. Sharonov. *Photochem. Photobiol.* **79**, 526 (2004).
27. D. Onidas, D. Markovitsi, S. Marguet, A. Sharonov, T. Gustavsson. *J. Phys. Chem. B* **106**, 11367 (2002).
28. A. L. Sobolewski, W. Domcke. *Phys. Chem. Chem. Phys.* **6**, 2763 (2004).
29. A. L. Sobolewski, W. Domcke, C. Hättig. *Proc. Natl. Acad. Sci.* **102**, 17903 (2005).
30. G. Groenof, L. V. Schäfer, M. Boggio-Pasqua, M. Goette, H. Grubmüller, M. A. Robb. *J. Am. Chem. Soc.* **129**, 6812 (2007).
31. D. Markovitsi, F. Talbot, T. Gustavsson, D. Onidas, E. Lazzarotto, S. Marguet. *Nature* **441**, E7 (2006).
32. J. Cadet, T. Douki, J. P. Pouget, J. L. Ravanat, S. Sauvaigo. *Curr. Prob. Dermat.* **29**, 62 (2001).
33. G. V. Buxton, C. L. Greenstock, W. P. Helman, A. B. Ross. *J. Phys. Chem. Ref. Data* **17**, 513 (1988).
34. L. P. Candeias, P. O'Neill, G. D. D. Jones, S. Steenken. *Int. J. Radiat. Biol.* **61**, 15 (1992).
35. D. N. Nikogosyan. *Int. J. Radiat. Biol.* **57**, 233 (1990).
36. H. Görner. *J. Photochem. Photobiol., B* **26**, 117 (1994).
37. M. Wala, E. Bothe, H. Görner, D. Schulte-Frohlinde. *J. Photochem. Photobiol., A* **53**, 87 (1990).
38. S. Marguet, D. Markovitsi, F. Talbot. *J. Phys. Chem. B* **110**, 11037 (2006).
39. S. Marguet, D. Markovitsi. *J. Am. Chem. Soc.* **127**, 5780 (2005).
40. W. J. Schreier, T. B. Schrader, F. O. Koller, P. Gilch, C. Crespo-Hernades, V. N. Swaminathan, T. Carell, W. Zinth, B. Kohler. *Science* **315**, 625 (2007).
41. W. M. Kwok, C. Ma, D. L. Phillips. *J. Am. Chem. Soc.* **130**, 5131 (2008).